Three-dimensional hydrodynamic focusing in a microfluidic Coulter counter

R. Scott,[1] P. Sethu,[2] and C. K. Harnett[1,a)]
[1]*Electrical and Computer Engineering Department, University of Louisville, Louisville, Kentucky 40208, USA*
[2]*Bioengineering Department, University of Louisville, Louisville, Kentucky 40208, USA*

(Received 30 September 2007; accepted 2 March 2008; published online 14 April 2008)

Electrical impedance-based particle detection or Coulter counting, offers a lab-on-chip compatible method for flow cytometry. Developments in this area will produce devices with greater portability, lower cost, and lower power requirements than fluorescence-based flow cytometry. Because conventional Coulter apertures are prone to clogging, hydrodynamic focusing improves the device by creating fluid-walled channels with variable width to increase sensitivity without the associated risk of blocking the channel. We describe a device that focuses the sample in three dimensions, creating a narrow sample stream on the floor of the channel for close interaction with sensing electrodes. The key to this design is a stepped outlet channel fabricated in a single layer with soft lithography. In contrast to previous impedance-based designs, the new design requires minimal alignment with the substrate. Three-dimensional focusing maximizes the sensitivity of the device to cell-size particles within much larger channels. Impedance-based particle sensing experiments within this device show an increase in percentage conductivity change by a factor of 2.5 over devices that only focus the sample in the horizontal direction. © *2008 American Institute of Physics.* [DOI: 10.1063/1.2900010]

Flow cytometry, a technique for analyzing cells suspended in a stream, is used in a variety of applications from fundamental biological research to drug development. However, current laser-based cytometers are confined to clinical and laboratory settings due to size, expense, power requirements, and need for skilled personnel.

There have been a few attempts to create a more portable optical cytometer but many involve miniaturizing the flow cell while preserving optical sources and detectors.[1–3] Therefore, these systems still possess some of the limitations of commercial cytometers.

Another approach, electrical impedance-based sensing or the Coulter technique, has been miniaturized in several recent papers.[4–10] Using this approach, the cell or particle sample is suspended in a conductive solution, causing a spike in resistance between the electrodes when a low-conductivity object interrupts the electrical path. Nanoscale particles have been detected using this approach when the minimum channel dimensions are comparable to the particle size.[5] However, this technique is only applicable to filtered solutions with particle sizes nearly equal to the channel width.

To minimize the risk of blockages in the device, soft fluid walls may be formed by coflowing low-conductivity side streams alongside the sample stream. Such hydrodynamic focusing has previously been combined with the micro-Coulter counter technique.[11,12] The method takes advantage of laminar flow in low-Reynolds number systems such as submillimeter width microfluidic channels. Hydrodynamic focusing reduces the width of the conductive sample stream to the approximate size of the sample particles, increasing the percentage resistance change in the conductive path when a particle passes by. Earlier work used two buffer streams on each side of the sample to achieve a focused stream with a minimum width of 2 μm.[11] However, this approach places the particle in the middle of a thin sheet of electrolyte, leaving conductive paths above and below the particle. Consequently, the channel depth still limits sensitivity. Since typical cell diameters are approximately 6–15 μm, the sample stream must still be tightly confined from top to bottom in a thin channel of height comparable to cell diameter for a detectable change in impedance.

Our device uses three-dimensional (3D) hydrodynamic focusing techniques to confine the sample stream in both the horizontal and vertical directions, creating a sensitive device that has all channel dimensions much greater than the particle diameter (in this work, 4.5–20 times greater). Vertical focusing can be accomplished with a two-level design for the channels in the device. The sample stream enters only on the bottom layer, while low-conductivity buffer enters from a channel that is both wider and taller than the sample stream. Low-conductivity buffer forms a sheath around the top and sides of the outlet channel, forcing the sample into a narrow stream at the bottom of the channel adjacent to the electrodes. Because the two-level mold's features can be captured in one cast elastomer piece, a single layer of elastomer can accomplish 3D focusing. Minimal alignment (+/−2 mm) is required to position the elastomer channel over a pair of thin-film metal electrodes on a glass substrate. Therefore, fabrication is less complicated than other techniques that require multiple layers of elastomer[13,14] or backside wafer alignment.[15] Our focusing technique is most similar to that used in a previous *optical* microcytometer,[2] the crucial

a)Author to whom correspondence should be addressed. Electronic mail: c0harn01@gwise.louisville.edu.

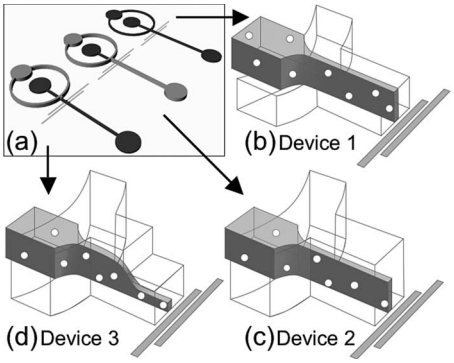

FIG. 1. (a) Schematic of the three flow cytometer designs built and tested. Dark gray regions are thin (typically 90 μm) and light gray regions are tall (typically 200 μm). (b) 2D focused flow device 1, showing a ribbon of particle-laden fluids crossing the sensing electrodes. (c) 2D focused flow device 2, which has a tall outlet channel. (d) 3D focused flow in device 3 is caused by stepping the outlet channel back down to the lower level.

difference being that we eliminate the lower sheath stream, placing the particles at the floor of the channel for close interaction with the impedance-sensing electrodes.

Devices were fabricated by casting silicone elastomer on a two-level mold made from SU-8 negative photoresist (MicroChem, Newton, MA, USA), and sealing the elastomer replicas to glass wafers that had been patterned with thin-film metal electrodes.

Three different device layouts [Figure 1(a)] included a single layer control device ["device 1," Fig. 1(b)], a two-level device that produces a particle stream of half the outlet channel height ["device 2," Fig. 1(c)], and a two-level device with a stepped outlet for full 3D focusing ["device 3," Fig. 1(d)]. Devices 2 and 3 each required two separate masks, one for each level in the mold.

The first layer of SU-8 50 was spun 90 μm thick and exposed to ultraviolet light through a photomask. The second layer of SU-8 was then applied for a combined thickness of 200 μm. The second mask was aligned with the visible cured features in the lower layer, and exposed. All unexposed resists were removed in propylene glycol monomethyl ether acetate. Consequently, the sample inlet and other features only in the first layer are roughly half of the height of the two-layer inlets and channels. The channel width is 100 μm (see Fig. 1). These relatively large channel dimensions were chosen to minimize the risk of clogging.

Microfluidic channels were replicated by casting polydimethylsiloxane (PDMS) elastomer (Sylgard 184, Dow Corning Corporation) over the mold.

Thin-film electrodes, with a typical edge-to-edge spacing of 25 μm, were patterned on a Pyrex wafer using photolithography. A 25–50 nm thick titanium adhesion layer was applied in a sputter deposition system followed by a 200 nm thick layer of platinum. Ti–Pt electrodes resist electrochemical corrosion and are biocompatible. The glass substrate is also biocompatible and provides good optical access for microscopy. Most importantly, its low conductivity improves the sensitivity of the device by minimizing leakage current through the substrate.

The PDMS was subsequently adhered to the patterned Pyrex wafer using a plasma activation and heat treatment process. After the Pyrex wafer was rinsed with water and dried, both Pyrex and PDMS bonding surfaces were treated in an air plasma cleaner (Harrick Plasma, Ithaca NY, USA) at 30 W and approximately 100 mTorr for 30 s. The PDMS and Pyrex surfaces were then aligned and pressed together and the devices were baked in an oven at 85 °C overnight, resulting in an irreversible and fluid-tight bond.

Wires were attached to the electrode bond pads using CircuitWorks CW2400 conductive epoxy. Tygon tubing was press fitted into holes punched in the ports of the device, producing a liquid-tight connection. Fluids were introduced from a syringe pump or gravity-driven reservoir. Side streams were supplied through one inlet port using a symmetrical T junction on the wafer.

Fluorescent polystyrene microbeads were used in our experiments as a low-conductivity particle with well-characterized diameter and good visibility in fluorescence microscopy. To prevent the beads from sedimenting, the sample was suspended in a density-matched aqueous sucrose solution (1 g sucrose/6.5 ml, 1.05 g/cm^3). Because this solution was essentially nonconductive, the sucrose solution in the center stream was formulated with 1 mM potassium chloride (KCl), raising its conductivity to 147 μS/cm. Two particle sizes were tested, representing the large and small ends of the size range for typical mammalian cells. Large particles were polystyrene 20 μm diameter yellow-green fluorescent particles (Bangs Labs, Inc., product FS07F) at 4.5×10^4 beads/ml of KCl solution and small particles were 6 μm diameter yellow-green fluorescent beads (Fluoresbrite Carboxy YG Microspheres, Polysciences, Inc., 18141) at 4×10^6 beads/ml of KCl solution. To match viscosity, the low-conductivity outer streams had the same sucrose concentration, without KCl.

A lock-in amplifier (SRS830, Stanford Research Systems) supplied a constant-amplitude sine wave across the electrodes and monitored the current, outputting a voltage directly proportional to the conductance between the electrodes. The applied signal had a typical peak-to-peak amplitude of 1 V and frequency of 30–50 KHz. A computer data acquisition signal sampled the lock-in output at 20 KHz, producing a time series of relative conductance values as particles flowed past the electrodes.

Confocal microscopy was performed to verify the location of the central stream in the two-level devices. Figure 2(a) is a top view of device 2, with 5 μM Texas red dye in sucrose solution pumped at 0.2 μl/min, and with side streams of undyed sucrose solution each flowing at 1 μl/min. This image was collected at approximately the halfway point in the device, 90 μm above the Pyrex substrate. Here and at points below, it closely resembles the flow pattern seen in device 1. Above 90 μm, however, the dye stream fades out, indicating that dye is excluded from the top of the device, as shown in Fig. 1(c). Figure 2(b) shows the dye stream at the level of the Pyrex substrate in device 3 under similar flow conditions. In contrast, Fig. 2(c) shows the flow in device 3 at a height of 90 μm. The dye stream enters the device as usual but when it encounters the step down to the lower level, undyed liquid pushes the dye stream down out of the focal plane, indicating that 3D hydrodynamic focusing has been achieved.

Figure 2(d) is a micrograph of device 3 showing focusing of 6 μm fluorescent beads in 5 μM Texas Red sucrose

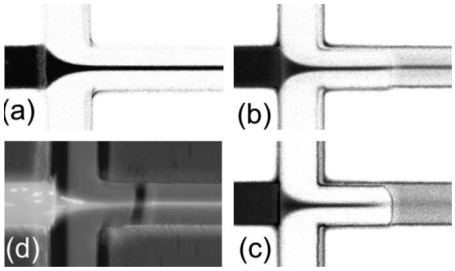

FIG. 2. Top-view microscope images of flow, contrasting 2D focusing in device 2 with 3D focusing caused by the step in device 3. In all cases, width of channels is 100 μm, central flow rate is in the range of 0.1 μl/min, side-stream flow rate 1 μl/min, and flow is from left to right. (a) Confocal slice of dye flow in device 2 at a height of 90 μm above the electrode plane. (b) Confocal slice of focused dye flow in device 3 at the electrode plane. (c) Confocal slice of dye flow in device 3 at 90 μm above the electrode plane; in contrast with (a), note that the outlet stream is diverted out of focus to the bottom of the channel by undyed fluid from above. (d) Fluorescence micrograph of 6 μm beads and dye in device 3 during a typical experiment.

solution. During the 140 ms shutter time, fast-moving beads in the focused stream appear as streaks, while individual slow-moving beads are visible in the entry channel.

Figure 3(a) shows a plot of the relative conductivity versus time for 20 μm beads in device 1, the two-dimensional (2D) hydrodynamically focused device. Flow rates were kept low in these experiments (1 μl/min for each side stream, 0.1 μl/min for the central stream). This led to a particle speed of 1.25 mm/s in the detection region, allowing visual confirmation of beads entering the detection channel. At this rate, the maximum throughput is 50 particles/s. In Fig. 3(a), the baseline conductivity, assigned the value 1, drops by as much as 0.5% while the bead is between the electrodes. Smaller drops are attributed to beads moving in streamlines higher above the electrodes. Such beads interrupt a smaller percentage of the current and typically have a faster transit time, as expected. In all experiments, gradual changes in relative flow rates of the sample and side streams create slow drift in the conductivity background signal, which we can distinguish from particle signals by high pass filtering. Figure 3(b) shows similar results for 20 μm beads in device 2. Both devices 1 and 2 produce a similar profile for the central

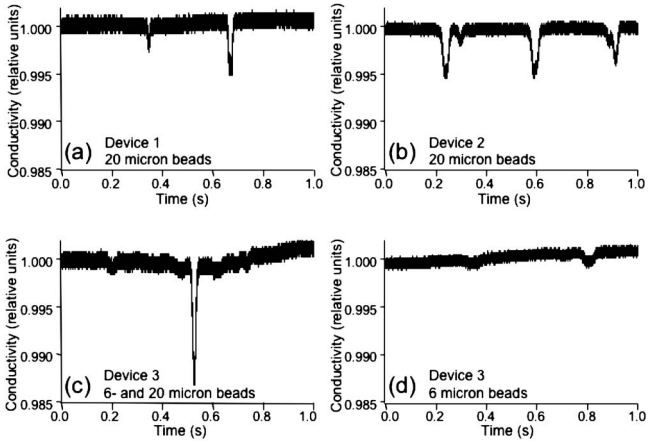

FIG. 3. Relative conductivity vs time plots for (a) 20 μm beads flowing in device 1, (b) 20 μm beads flowing in device 2, (c) 20 and 6 μm beads flowing in device 3, and (d) 6 μm beads flowing in device 3.

stream, as illustrated in Fig. 1; the main advantage of device 2 is that it has a tall outlet channel, reducing flow resistance and the likelihood of clogging.

Figure 3(c) shows a maximum 1.25% decrease in conductivity, 2.5 times larger than the conductivity decrease observed in devices 1 and 2, as a mixture of 6 μm diameter and 20 μm diameter beads pass through device 3. The sharp drop in conductivity is attributed to a 20 μm bead observed entering the device during data collection, while new small fluctuations are attributed to the 6 μm beads, which were not observable in devices 1 and 2. Figure 3(d) shows a 0.2% conductivity decrease when 6 μm beads alone are flowed through the device. Device 3 produces greater changes in conductivity than both previous devices.

In summary, we have presented a design for a micro-Coulter counter with a stepped outlet channel, which demonstrates a 2.5 times increase in signal strength over a non-stepped device, due to hydrodynamic focusing in both horizontal and vertical directions. The device is fabricated using simple techniques that require a minimal amount of alignment. Using a standard PDMS process also enables multiple devices to be created from one SU-8 mold.

Results distinguishing particles down to 6 μm in diameter within the focused sample stream are shown. The performance of our 3D device is favorably compared to a 2D control device that uses the technique of focusing the sample into a thin sheet. The 3D device was more sensitive and was able to detect cell-size particles with channel width and height at least 15 times the particle diameter, minimizing the risk of creating a blockage in the channel.

Future work involves modifying the electrical characteristics of the particles/cells so that the impedance sensor can also sense the chemical state of the cell surface. Modifications include tagging cells with conductive and insulating particles through antibody-antigen interactions.

We thank Mark Crain, Joseph Lake, Don Yeager and Arkadiusz Slusarczyk at the University of Louisville.

[1] R. Bernini, E. De Nuccio, F. Brescia, A. Minardo, L. Zeni, P. Sarro, R. Palumbo, and M. Scarfi, Anal. Bioanal. Chem. **386**, 1267 (2006).
[2] C. Simonnet and A. Groisman, Anal. Chem. **78**, 5653 (2006).
[3] D. Spicer, J. McMullin, and H. Rourke, J. Micromech. Microeng. **16**, 1674 (2006).
[4] M. Koch, A. Evans, and A. Brunnschweiler, J. Micromech. Microeng. **9**, 159 (1999).
[5] O. Saleh and L. Sohn, Rev. Sci. Instrum. **72**, 4449 (2001).
[6] J. Zhe, A. Jagtiani, P. Dutta, H. Jun, and J. Carletta, J. Micromech. Microeng. **17**, 304 (2007).
[7] D. K. Wood, M. V. Requa, and A. N. Cleland, Rev. Sci. Instrum. **78**, 104301 (2007).
[8] S. Gawad, L. Schild, and Ph. Renaud, Lab Chip **1**, 76 (2001).
[9] H. Morgan, T. Sun, D. Holmes, S. Gawad, and N. Green, J. Phys. D **40**, 61 (2007).
[10] K. Cheung, S. Gawad, and P. Renaud, Cytometry **65A**, 124 (2005).
[11] R. Rodriguez-Trujillo, C. Mills, J. Samitier, and G. Gomila, Microfluid. Nanofluid. **3**, 171 (2007).
[12] P. Walsh, E. Walsh, and M. Davies, Int. J. Heat Fluid Flow **28**, 44 (2007).
[13] N. Sundararajan, M. Pio, L. Lee, and A. Berlin, J. Microelectromech. Syst. **13**, 559 (2004).
[14] C.-C. Chang, Z.-X. Huang, and R.-J. Yang, J. Micromech. Microeng. **17**, 1479 (2007).
[15] J. Nieuwenhuis, F. Kohl, J. Bastememeijer, P. Sarro, and M. Vellekoop, Sens. Actuators B **102**, 44 (2004).